Identification and characterization of a novel FBN1 gene variant in an extended family with variable clinical phenotype of Marfan syndrome

Identification and characterization of a novel *FBN1* gene variant in an extended family with variable clinical phenotype of Marfan syndrome

Mahmut Cerkez Ergoren[1], Burcu Turkgenc[2], Kerem Teralı[3], Orhan Rodopluu[4], Aline Verstraeten[5], Lut Van Laer[5], Gamze Mocan[6], Bart Loeys[5], Omer Tetik[7], Sehime G Temel[8,9,10]

[1] Department of Medical Biology, Faculty of Medicine, Near East University, Nicosia, Cyprus

[2] Acibadem Diagnostic Center, Istanbul, Turkey

[3] Department of Medical Biochemistry, Faculty of Medicine, Near East University, Nicosia, Cyprus

[4] Private Yalova Specilaists' Hospital, Yalova, Turkey

[5] Center for Medical Genetics, Antwerp University Hospital/University of Antwerp, Antwerp, Belgium

[6] Department of Pathology, Faculty of Medicine, Near East University, Nicosia, Cyprus

[7] Department of Cardiovascular Surgery, Celal Bayar University, Manisa, Turkey.

[8] Department of Histology and Embryology

[9] Department of Medical Genetics, Uludağ University, Bursa, Turkey.

[10] Department of Histology & Embryology, Faculty of Medicine, Near East University, Nicosia, Cyprus

Competing interest

The authors state that the research has been performed in an environment where there are no commercial or financial relationships that could be interpreted as a possible conflict of interest.

Introduction

Marfan syndrome (MFS) is a rare (1:3000 to 1:5000 incidence in the general population) autosomal dominant connective tissue disorder with variable expressivity of clinical features in the musculoskeletal, cardiovascular and ocular systems (1). Tall stature with long limbs, arachnodactyly, pectus excavatum or carinatum, scoliosis, protrusion acetabuli, pes plani, muscle hypotonia and a long face are frequently observed in individuals with MFS. Mitral valve prolapses, pneumothorax, dural ectasia, ectopia lentis and myopia are common too. Aortic aneurysm/dissection is an important final hallmark, as aortic dissection represents the major cause of mortality in MFS (2). Of note, significant phenotypic variability has regularly been observed between affected members of different families or even within families (3).

Deficiency for fibrillin-1 (encoded by *FBN1)* is the underlying cause of MFS. *FBN1*, which consists of 65 exons, is located on chromosome 15q21.1 and encodes a secreted 350-kDa extracellular matrix glycoprotein that is an essential, structural component of calcium-binding microfibrils (4). Fibrillin-1 mostly consists of epidermal growth factor (EGF)-like domains (5). 43 out of the 47 EGF-like domains in human fibrillin-1 start with the conserved D-X-D/N-E motif which is involved in calcium binding (hence called cbEGF-like domains). Calcium binding to fibrillin-1 has been shown to provide structural stabilization, protection against proteolysis, and structural determinants for interaction with a number of elements of the extracellular matrix (reviewed in 6). In each cbEGF-like domain, stability is further mediated by establishment of three disulfide bonds that interconnect six evolutionary conserved cysteine residues in a pairwise manner (7,8).

The most extensive *FBN1* mutation database (http://umd.be/FBN1/-latest update 28/08/2014) contains 1847 different mutations in 3044 patient samples (9). Mutations are widespread throughout the gene and only 12% of all reported *FBN1* mutations are recurrent (8). Unfortunately, the current mutation databases do not offer sufficient clinical and mechanistic data for establishing specific genotype–phenotype correlations between the identified *FBN1* mutations and variable expressivity of the symptoms of MFS. Establishment of genotype–phenotype correlations is further hampered by the age-related nature of some clinical symptoms as well as the variable phenotype of MFS (20). Nonetheless, a relatively significant amount of research is ongoing to refine the very complex genotype–phenotype association in MFS patients from different families as well as from the same family, who are known to carry *FBN1* mutations.

Previous studies showed that affected family members bearing the same *FBN1* mutation often presented the same phenotype (20). Here, we detected a heterozygous *FBN1*

variation (c.7828 G>C in exon 64; p.Glu2610Gln) in nine family members from a five-generation pedigree associated with variable and different clinical features. Furthermore, we developed an *in silico* model to gain a better understanding of the mechanistic and structural aspects of the p.Glu2610Gln variation situated in the human fibrillin-1 cbEGF-like domain 42.

Materials and methods

Patients and clinical data

A five-generation pedigree (Figure 1A) with MFS was recruited from the Department of Cardovascular Surgery in Yuksek Ihtisas Hospital in Bursa, Turkey. All the family members in the present study were diagnosed within the same department of the hospital. This study was approved by the Medical Ethics Committee of the Yuksek Ihtisas Hospital, Bursa, Turkey. Written informed consent was obtained from all the subjects or their legal guardians.

The personal medical history and the family medical history of each family member were thoroughly reviewed. Additionally, all participants underwent physical, ophthalmological, radiological and cardiovascular examinations. All the MFS patients were diagnosed according to the revised Ghent criteria (21).

Clinical data and peripheral blood samples were collected from nine affected (III:1, III:7, III:9, IV:4, IV:6, IV:10, IV:14, IV:15, and IV:17) and nine unaffected family members (III:5, IV:1, IV:2, IV:5, IV:8, IV:9, IV:11, IV:12, IV:13, and IV:16). Family members designated IV:2, IV:3, and V:1 could not be investigated personally due to the fact that they currently live in France.

Molecular analyses

Genomic DNA was extracted for targeted next-generation sequencing at the Center of Medical Genetics in Antwerp. A HaloPlex gene panel (Agilent Technologies, USA) was used to selectively capture known syndromic and non-syndromic aneurysmal genes (22). This panel includes *ACTA2* (NM_001141945), *COL3A1* (NM_000090), *FBLN4* (NM_016938), *FBN1* (NM_000138), *FLNA* (NM_001110556), *MYH11* (NM_022844), *MYLK* (NM_053025), *PRKG1* (NM_006258), *SKI* (NM_003036), *SLC2A10* (NM_030777), *SMAD3* (NM_005902), *TGFB2* (NM_001135599), *TGFBR1* (NM_004612), and *TGFBR2* (NM_003242). The targeted fragments were then sequenced on a MiSeq platform (Illumina, USA) and data analysis was performed with the in-house developed automated data analysis pipeline and variant interpretation tool VariantDB. The significance of the variant was

determined according to: (i) the nature of the variant and its position; (ii) the presence of these variants in the ExAC and dbSNP databases; and (iii) their impact on the structure and function of the resulting protein. Finally, Sanger sequencing was performed to validate the identified mutation and to investigate familial segregation patterns.

Histological, pathological and immunohistochemical analyses

Periodic acid-Schiff with Alcian blue (PAS–AB) and van Gieson staining protocols were applied to the paraffin-embedded sections of the aorta of the proband (III-7) and of the proband's brother (III-1). Immunohistochemical staining was subsequently performed with a fibrillin-1 antibody (1:50, sc-20084, Santa Cruz Biotechnology, Inc., Santa Cruz, CA) in the paraffin-embedded sections of the aorta of the proband (III-7), proband's brother and a control aorta of age and sex matched forensic case Who deceased because of trauma, available in the Ministry of Justice, Council of Forensic Medicine, Mortuary Department, Istanbul, Turkey

***In silico* protein analysis**

The information regarding the primary protein sequence and domain boundaries of human fibrillin-1 was obtained from the UniProt Knowledgebase http://www.uniprot.org/; entry: P35555). The minimized average nuclear magnetic resonance (NMR) structure of a covalently linked pair of human fibrillin-1 cbEGF-like domains were downloaded from the Protein Data Bank (http://www.rcsb.org/; entry: 1EMN), and profiling of the noncovalent interactions between the cbEGF-like domains and Ca^{2+} ions was performed by using the PLIP Web service (23). A comparative model of the covalently linked cbEGF-like domains no. 41 (residues 2567–2606) and no. 42 (residues 2607–2647) was built based on the 1EMN template by using the CPHmodels, Version 3.2 protein homology modeling server (24). The p.Glu2610Gln substitution was introduced *in silico* by using the Mutagenesis Wizard of the PyMOL Molecular Graphics System, Version 1.8 (Schrödinger, LLC, Portland, OR, USA), adopting the Gln side-chain rotamer with a closely similar conformation to that of the Glu side-chain rotamer, as well as with virtually no steric clashes with other amino acid side chains or the main-chain atoms of the protein.

Results

Clinical findings of the pedigree

The 37-year-old male propositus (III:7) ***(Figure 1A)*** was referred to the Department of Cardiovascular Surgery, Yuksek Ihtisas Hospital, Bursa, Turkey because of chest pain and shortness of breath. The major clinical findings of the propositus included severe myopia, lens subluxation, and mild marfanoid facial features (Figure 1B). Echocardiography and computerized tomography (CT) (Figure 1C) revealed chronic type I aortic dissection, an ascending aortic aneurysm at sinus valsalva level (90 mm) and severe aortic valve insufficiency. His family medical history was significant for sudden death; his father and older sister died at ages of 51 and 36 years, respectively, and variable phenotypes were observed in three generations of the family (Figure 1D). The proband's older (age of 41 years) brother (III:1) presented with severe chest abnormalities (pectus carinatum, Figure 1E), myopia-astigmatism, and lens subluxation. His echocardiography and CT (Figure 1F) similarly demonstrated chronic type I aortic dissection, an ascending aortic aneurysm at sinus valsalva level (70 mm), and severe aortic valve insufficiency. The two brothers underwent immediate Bentall procedure.

Upon further work-up of the family, echocardiography results indicated a 38-mm aortic root diameter at sinus valsalva level in the proband's 38-year-old sister (III:9). She also had mild pectus carinatum and lens subluxation. The main clinical findings of 26-year-old IV:5 were mild pectus carinatum (Figure 1G), myopia-astigmatism, and lens subluxation. His echocardiography and CT results demonstrated a dilated aortic root (42 mm) (Figure 1H).. The 12-year-old female (IV:7) presented with mild chest deformity and tall stature (165 cm, 96.9 percentile), and her echocardiography results showed a 35-mm aortic root diameter at sinus valsalva level. Clinical features of IV:10 (age of 18 years) included severe pectus carinatum, tall stature (193 cm, 99.2 percentile), and normal aortic diameters at sinus valsalva level upon echocardiography. IV-14 (age of 17 years) and IV-15 (age of 15 years) presented tall stature (196, 99.8 percentile and 180 cm, 99.8 percentile respectively) with skeletal abnormalities (chest asymmetry with pectus carinatum) and myopia. Echocardiographies of IV:14, IV:15 and IV:17 revealed normal aortic diameters at ages 15, 17 and 7 respectively. Taken together, cardiovascular disease was strikingly more severe in III:1 and III:7 compared to the other affected family members.

Molecular genetic analyses

Aneurysm gene panel analysis for the proband (III:7) and subsequent segregation analysis in all affected family members (III:1, III:7, III:9, IV:4, IV:6, IV:10, IV:14, IV:15, and IV:17) revealed the presence of a heterozygous missense variant (c.7828 G>C; p.Glu2610Gln) in exon 64 of the *FBN1* (NM 000138) gene (Figure 2). This heterozygous variant was absent in

the nine family members (III:5, IV:1, IV:2, IV:5, IV:8, IV:9, IV:11, IV:12, IV:13, and IV:16) lacking diagnostic features of MFS. As such, the variant is fully co-segregating with the disorder in the family and unequivocally associated with the phenotype. Importantly, this variation has not previously been reported on the national Turkish control database (TUBITAK/BILGEM; 2100 individuals). However, in the Universal Mutation Database (UMD)-*FBN1*, this variation was reported once, but no phenotypical details were provided (personal communication by Prof. Boileau). Communication with Prof. Boileau and Dr. Nadine Hanna revealed that this patient shared the same Turkish name and surname as well as a similar medical history as the proband (III:9) in our pedigree. It is worth mentioning, though, that this variation has not been reported in the relevant scientific literature before. The p.Glu2610Gln mutation affects the highly conserved glutamate residue from the DINE-consensus sequence of cbEGF domain no.42 of fibrillin-1. While the UMD-predictor states that this variant is a polymorphism, other *in silico* prediction tools, such as PolyPen-2 (25), SIFT (26), Mutation Taster, (27), and Mutation Assessor (28), identify this heterozygous variant as pathogenic.

Pathological, histological and immunohistochemical findings

In the proband's aorta (III-7), elastic fiber degeneration and fragmentation versus normal age matched control aorta, x20, respectively (Figure 3A, 3C), myxoid medial inclusion (Figure 3D), and, in one area, dissection of the media was observed. Similar findings were also observed in the aorta of the proband's brother (III-1) (Figure 3B, 3E).

Immunohistochemistry for fibrillin-1 showed decreased protein expression in the proband's (III-7) (Figure 3F) and proband's brothers' (III-1) (Figure 3G) aorta compared to normal staining throughout the aorta of age and sex matched control (Figure 3H)).

***In silico* protein analysis**

With an amino acid sequence identity of 43.8% to the covalently linked cbEGF-like domains no. 41 and no. 42 (the latter of which bears the site of substitution), the NMR structure of the adjacent cbEGF-like domains no. 32 and no. 33 (PDB ID: 1ENM) proved to be a good template for protein comparative modeling (Figure 4A). Protein–ligand interaction profiling analysis of this structure revealed that each Ca^{2+} ion formed a five-coordinated metal complex with a trigonal bipyramidal geometry (Figure 4B). More importantly, two of these five coordination bonds were established with the side-chain carbonyl and side-chain hydroxyl oxygens of the Glu residue of the conserved D-X-D/N-E motif. The same bonding pattern was

also observed in the structure of the predicted cbEGF-like 41–42 fragment, supporting the validity of our protein comparative model (Figure 4C). *In silico* mutation of Glu-2610 to Gln demonstrated that the side chain of Gln could also be accommodated readily in the Ca^{2+}-binding site, in a similar rotamer conformation to that of Glu in the wild-type protein (Figure 4D).

Discussion

MFS is clinically characterized by manifestations of multiple organ systems, including the cardiovascular, ocular, and skeletal systems. Cardiovascular complications such as aortic root aneurysm and aortic dissection are the most life-threatening manifestations of MFS (29).

In 1991, *FBN1* was identified as the only gene associated with the pathogenesis of MFS (11). To date, nearly 2000 unique *FBN1* mutations have been reported to cause MFS (9). The location of the mutations is widespread over the gene, and most of them are unique to each family. The mutational spectrum of *FBN1* encompasses all possible types of mutations including stop codons, splice site mutations, insertions/deletions and missense variations, as well as multi-exon and whole-gene deletions (30, 31).

Few strong genotype–phenotype correlations have emerged, though it has been noted that mutations in different exons of *FBN1* can produce variable phenotypes (19, 30, 32, 39). Patients carrying *FBN1* mutations in exons 1–21 have been reported to frequently show ectopia lentis (80%) while mutations in exons 23–32 likely come with aortic root dilation (33). On the contrary, mutations in exons 1–10 were found to be associated with no cardiovascular complications (32) and mutations in exons 59–65 were found to be linked with milder MFS-like phenotypes (34). The vast majority of the mutations in the middle region of the gene (exons 24–32) are related to severe neonatal Marfanoid manifestations according to previous observations, but some exceptions have been reported (35, 36). Besides the location of the mutation, also the type of mutation has been reported to impact on disease severity. One of the first genotype–phenotype correlation reports found an enrichment of missense mutations involving cysteine residues in MFS cases with ectopia lentis in a cohort of 104 MFS cases (36). These ocular findings were confirmed by two other reports (37, 38). Aortic dissections appeared to be more common in cases with premature stop codon mutations compared to cysteine-deleting or creating mutation carriers, but this has not been unequivocally replicated. Faivre *et al.* (2012) were the ones who published data from the largest genotype–phenotype MFS study (1013 independent MFS probands) (39). In their cohort, skeletal and skin involvement was seen more frequently in patients carrying a stop codon mutation. The cumulative probability of a diagnosis of ascending aortic dilatation

before or at age 40 years was 77% for patients with premature termination codon mutations compared with 74% for patients with an in-frame mutation. In contrast, the cumulative probability of a diagnosis of ectopia lentis was significantly lower for patients with premature termination codon mutations compared with patients with an in-frame mutation. A recent smaller cohort demonstrated that truncating and splice-altering mutations more abundantly correlate with aortic events at young ages (40). Not long ago, Franken *et al.* (2017) tracked aortic diameter, aortic dilation rate and clinical endpoints of dissection and death from 2004 to 2015 in 290 patients with MFS from Spain and the Netherlands (53). Their analysis revealed that fibrillin-1 haplo-insufficiency mutation carriers had a more severe aortic phenotype, with larger aortic root diameters and a more rapid dilation rate, and tended to have an increased risk of sudden death and dissections compared with fibrillin-1 dominant-negative mutation carriers (53).

We identified a missense mutation (p.Glu2610Gln) in a large MFS family with significant variability with respect to disease severity. Although the mutation is located in exon 64 and does not involve a cysteine residue, four of the affected family members (III-1, III-7, III-9, IV-1) have lens subluxation and two (III-1 and III-7) presented with a giant ascending aortic aneurysm (70 and 90 mm, respectively) and severe aortic valve insufficiency requiring Bentall surgery. The manifestation of aortic root dilatation is severe but not early-onset. Additionally, affected family members have skeletal abnormalities ranging from mild to severe but mostly account for the mild type.

In a structural context, the p.Glu2610Gln substitution detected in our family is likely to cause a minimal perturbation to the local protein structure due to the fact that Glu and Gln are similar in hydrophilicity, α-helical propensity and spatial requirements (42). From a functional perspective, however, the substitution is predicted to hinder Ca^{2+} binding because of the loss of one of the metal-coordinating oxygens. It has been suggested that mutations affecting Ca^{2+}-binding residues have short- and long-range repercussions on the fate of fibrillin-1 (7). For instance, the engineered p.Glu1073Lys substitution in the cbEGF-like domain no. 12, which has previously been shown to be associated with the neonatal form of MFS (34), was found to cause increased proteolytic susceptibility with newly introduced cleavage sites both in close proximity to the mutated residue and within the EGF-like domain no. 4 and cbEGF-like domains no. 3, no. 11 and no. 17 (44, 45). Overall, we suggest that the p.Glu2610Gln substitution impairs the ability of the C-terminal portion of fibrillin-1 to bind Ca^{2+}, possibly leaving the mutant protein vulnerable to proteases. We do not, however,

exclude the possibility that this substitution may, alternatively, disrupt the interplay between fibrillin-1 and its interacting partners or affect fibrillin-1 secretion.

MFS has been characterized by clinical heterogeneity among individuals with the same mutation, within and among families like seen in our family (19, 47, 48). The nature or location of the *FBN1* mutation alone cannot explain this variation. These observations suggest the existence of other genetic or environmental modifiers explaining the variable susceptibility of micro-fibrillar matrices to proteolytic degradation. Alternatively, intra-familial variation in fibrillin-1 biosynthesis may account for the variable *FBN1* mutant phenotype (49, 50). As a possible explanation, it has been speculated that differences in wild-type *FBN1* expression levels account for this intra-familial clinical variability (50-52). In our family, aortic tissues of III-1 and III-7 were available, and fibrillin-1 expression was assessed by immunohistochemistry. Fibrillin-1 was totally diminished in both their aortic tissues, but they both additionally had a highly severe aortic phenotype. The other affected family member's tissue samples were not available to show the clinical variability in fibrillin-1 expression levels.

Scientist examined 290 patients with MFS and known *FBN1* mutations at the two specialist units, one in Spain and the other in the Netherlands (52). Franken *et al.* (2017) tracked aortic diameter, aortic dilation rate and clinical endpoints of dissection and death from 2004 to 2015. Concluding that haploinsufficiency mutation carriers had a more severely affected aortic phenotype, with larger aortic root diameters and a more rapid dilation rate and tended to have an increased risk of death and dissections compared with patients with an inclusion of non-mutated and mutated fibrillin-1 in the extracellular matrix (52).

Despite the fact that MFS shows autosomal dominant inheritance, the disease has widespread phenotypic variability in, for instance, the age of onset, severity and the progression of aortic aneurysm. Regrettably, genotype–phenotype correlations are currently unpredictable for individuals or families, putting major obstacles in the way of clinicians directly responsible for taking critical decisions. Because of that reason, timely differential diagnosis is extremely important for early diagnosis and intervention of aneurysms to prevent serious vascular complications in MFS and Marfan-related disorders.

Consent for publication: Consents for publication from all families were obtained. All the patient's guardians provided informed consent for publication of the submitted article, and the results of the accompanying genetic analyses, after a full explanation of the purpose and nature of all the procedures used.

Funding

This study was supported by the Center of Excellence of Near East University CE010-2015

.

Decleration of interest

The authors report no conflicts of interest.

Acknowledgements

The authors wish to express their gratitude to the family members for participating in this study.

Figure legends

Figure 1 **Pedigree and clinical findings of the Turkish family with MFS.** (**A**) Pedigree of the family. Squares indicate males and circles indicate females. The filled symbols represent the patients with the heterozygous p.Glu2610Gln mutation within the *FBN1* gene. The arrow indicates the propositus. Question marks indicate unknown genotypic data on the *FBN1* gene for those patients. (**B**) Proband's mild marphanoid facial features and severe myopia. (**C**) Proband's CT results show the ascending aneurismatic aorta (dark blue asterisk), true (red asterisk) and false (black asterisk) lumen in descendent aorta (**D**) Variable clinical expression of Marfan phenotype in the family. (**E**) Severe pectus carinatus of the proband's brother (III-1). (**F**) True (red asterisk) and false (black asterisk) lumen in aorta of the proband's brother (III-1). (**G**) Mild pectus carinatus of the proband's nephew (IV-5). (H) Proband's nephew (IV-5) CT results show ascending (black asterisk) dilated aorta (descending aorta/red asterisk).

Figure 2 **DNA sequencing results of the heterozygous carriers and non-carriers and multiple sequence alignment results of the *FBN1* variant.** (**A**) DNA sequencing results of heterozygous carrier of the c.7828 G>C (p.Glu2610Gln) variant. (**B**) DNA sequencing results of an unaffected family member. (**C**) Multiple sequence alignment results of the *FBN1* variant across different species based on the PolyPhen-2 tool.

Figure 3 **Van Gieson staining, PAS–AB staining and immunohistochemistry results. Lumen is always oriented to the top.** (**A**) Elastic fibril degeneration in the proband's and **(B)** in the proband's brother's aorta, and normal elastic fiber organization in normal aorta, ×20

(C) (by van Gieson staining). **(D)** Myxoid degeneration in the tunica media and interstitium of the proband's, and in the proband's brothers' aorta section, ×40 **(E) (**by PAS–AB staining). **(F)** Immunohistochemistry results for fibrillin-1 show decreased protein production in the proband's aorta (III-7), ×40, and in the proband's brothers' aorta, ×40 **(G)**, normal levels of fibrillin-1 immunostaining throughout the aorta of age- and sex-matched control case, ×40 **(H).**

Figure 4 In silico **analysis of the mutant fibrillin-1 molecule.** (**A**) Solution structure of the covalently linked human fibrillin-1 cbEGF-like domains no. 32 and no. 33 (PDB ID: 1EMN). The carbon atoms of the protein fragment are shown as brown sticks, and the two bound Ca^{2+} ions are shown as magenta spheres. Hydrogen atoms are not shown for clarity. The figure was rendered using the PyMOL Molecular Graphics System, Version 1.8 (Schrödinger, LLC, Portland, OR, USA). (**B**) Close-up view of the interaction between human fibrillin-1 cbEGF-like domain no. 33 and the Ca^{2+} ion. The metal ion is held in place by five coordination bonds, two of which have been calculated to involve Glu-2169 of the conserved D-X-D/N-E motif. The carbon atoms of the calcium-binding residues are shown as brown sticks, the Ca^{2+} ion is shown as a magenta sphere, and the metal coordination bonds are shown as magenta dashed lines. Protein–ligand interaction profiling was performed using PLIP (Salentin *et al.*, 2015), and the figure was rendered using the PyMOL Molecular Graphics System, Version 1.8 (Schrödinger, LLC, Portland, OR, USA). (**C**) Cartoon representation of the cbEGF-like 41–42 domain pair comparative model. The domain no. 41 is shown in green, and the domain no. 42 is shown in blue. Glu-2610, which appears to be located on the edge of a short α-helix, is shown as sticks. The two Ca^{2+} ions, which have been added to the model after alignment of the determined and predicted structures, are shown as magenta spheres. The image was rendered using the PyMOL Molecular Graphics System, Version 1.8 (Schrödinger, LLC, Portland, OR, USA). (**D**) Close-up view of the *in silico* introduced p.Glu2610Gln mutation. The carbon atoms of the side chain of Glu-2610 are shown as blue sticks, and the carbon atoms of the best-selected side-chain rotamer of Gln-2610 are shown as gray sticks. The Ca^{2+} ion is shown as a magenta sphere. The figure was rendered using the PyMOL Molecular Graphics System, Version 1.8 (Schrödinger, LLC, Portland, OR, USA).

References:

1. Keane M.G., Pyeritz R.E. Medical management of Marfan syndrome. Circulation 117; 2802–2813, 2008.
2. Yang H., Luo M., Chen Q., Fu Y., Zhang J., Qian X., Sun X., Fan Y., Zhou Z., Chang Q.Genetic testing of the FBN1 gene in Chinese patients with Marfan/ Marfan-like syndrome. Clinica Chimica Acta 459; 30-35, 2016.
3. Dietz H.C., Pyeritz R.E., Mutations in the human gene for fibrillin-1 (FBN1) in the Marfan syndrome and related disorders. Hum. Mol. Genet 4 Spec No: 1799-1809, 1995.
4. Ramirez F., Sakai L.Y. Biogenesis and function of fibrillin assemblies. Cell Tissue Res 339;71–82, 2010.
5. Pereira, L., D'Alessio, M., Ramirez, F., Lynch, J.R., Sykes, B., Pangilinan, T., Bonadio, J. (1993). Genomic organization of the sequence coding for fibrillin, the defective gene product in Marfan syndrome, *Human Molecular Genetics*, 2(7), 961–968. DOI: 10.1093/hmg/2.7.961
6. Zeyer, K.A., Reinhardt, D.P. (2015). Engineered mutations in fibrillin-1 leading to Marfan syndrome act at the protein, cellular and organismal levels. *Mutation Research/Reviews in Mutation Research*, 765, 7–18. DOI: 10.1016/j.mrrev.2015.04.002
7. Downing A.K., Knott V., Werner J.M., Cardy C.M., Campbell I.D., Handford P.A. Solution structure of a pair of calcium-binding epidermal growth factor-like domains: implications for the Marfan syndrome and other genetic disorders. Cell 85;597–605, 1996.
8. Schrijver I., Liu W., Brenn T., Furthmayr H., Francke U. Cysteine substitutions in epidermal growth factor-like domains of fibrillin-1: distinct effects on biochemical and clinical phenotypes, Am. J. Hum. Genet 65;1007–1020, 1999.
9. http://www.umd.be/FBN1/
10. Collod-Béroud G., Le Bourdelles S., Ades L., Ala-Kokko L., Booms P., Boxer M., Child A., Comeglio P., De Paepe A., Hyland J.C., Holman K., Kaitila I., Loeys B., Matyas G., Nuytinck L., Peltonen L., Rantamaki T., Robinson P., Steinmann B., Junien C., Béroud C., Boileau C. Update of the UMD-FBN1 mutation database and creation of an FBN1 polymorphism database. Hum. Mutat 22;199–208, 2003.
11. Dietz H.C., Cutting G.R., Pyeritz R.E., et al. Marfan syndrome caused by a recurrent de novo missense mutation in the fibrillin gene. Nature 352;337–339, 1991.

12. Zhang L., Lai Y.H., Capasso J.E., Han S., Levin A.V. Early onset ectopia lentis due to a FBN1 mutation with non-penetrance, Am. J. Med. Genet A 167;1365–1368, 2015.
13. Edwards M.J., Challinor C.J., Colley P.W., et al. Clinical and linkage study of a large family with simple ectopia lentis linked to FBN1. Am. J. Med. Genet 53;65–71, 1994.
14. Hoffjan S. Genetic dissection of marfan syndrome and related connective tissue disorders: an update 2012, Mol. Syndromol 3;47–58, 2012.
15. Bergman R., Nevet M.J., Gescheidt-Shoshany H., Pimienta A.L., Reinstein E. Atrophic skin patches with abnormal elastic fibers as a presenting sign of the MASS phenotype associated with mutation in the fibrillin 1 gene. JAMA Dermatol 150;885–889, 2014.
16. Fu Q., Liu P., Lu Q., et al. Novel mutation in FBN1 causes ectopia lentis and varicose great saphenous vein in one Chinese autosomal dominant family. Mol. Vis 20;812–821, 2014.
17. Hayward C., Brock D.J. Fibrillin-1 mutations in Marfan syndrome and other type-1 fibrillinopathies. Hum. Mutat 10; 415–423, 1997.
18. Katsuragi S., Neki R., Yoshimatsu J., Ikeda T., Morisaki H., Morisaki T. Acute aortic dissection (Stanford type B) during pregnancy. J. Perinatol 33;484–485, 2013.
19. Loeys B., Nuytinck L., Delvaux I., De Bie S., De Paepe A. Genotype and phenotype analysis of 171 patients referred for molecular study of the fibrillin-1 gene FBN1 because of suspected Marfan syndrome. Arch. Intern. Med 161;2447–2454, 2001.
20. Milewicz D.M., Grossfield J., Cao S.N., Kielty C., Covitz W., Jewett T. A mutation in FBN1 disrupts profibrillin processing and results in isolated skeletal features of the Marfan syndrome. J Clin Investig 952373-2378, 1995
21. Loeys BL, Dietz HC, Braverman AC, Callewaert BL, De Backer J, Devereux RB, Hilhorst-Hofstee Y, Jondeau G, Faivre L, Milewicz DM, Pyeritz RE, Sponseller PD, Wordsworth P, De Paepe AM. The revised Ghent nosology for the Marfan syndrome. J Med Genet. 2010 Jul;47(7):476-85
22. Proost D, Vandeweyer G, Meester JA, Salemink S, Kempers M, Ingram C, Peeters N, Saenen J, Vrints C, Lacro RV, Roden D, Wuyts W, Dietz HC, Mortier G, Loeys BL, Van Laer L. Hum Mutat. 2015;36(8):808-14. Performant Mutation Identification Using Targeted Next-Generation Sequencing of 14 Thoracic Aortic Aneurysm Genes.

23. Salentin, S., Schreiber, S., Haupt, V.J., Adasme, M.F., Schroeder, M. (2015). PLIP: fully automated protein–ligand interaction profiler. *Nucleic Acids Research*, 43(W1), W443–447. DOI: 10.1093/nar/gkv315
24. Nielsen, M., Lundegaard, C., Lund, O., Petersen, T.N. (2010). CPHmodels-3.0—remote homology modeling using structure-guided sequence profiles. *Nucleic Acids Research*, 38(suppl_2), W576–581. DOI: 10.1093/nar/gkq535
25. http://genetics.bwh.harvard.edu/ggi/pph2/c51a79199723f32f490405ed277312b9b23d8894/3942946.html
26. http://provean.jcvi.org/protein_batch_view_table.php?jobid=085036761895700
27. http://www.mutationtaster.org/cgi-bin/MutationTaster/MutationTaster69.cgi
28. http://mutationassessor.org/r3/.
29. Liu D.L., Cao J.H., Yang J. et al., A novel mutation in fibrillin-1 gene identified in a Chinese family with marfan syndrome. Int. J. Clin. Exp. Med. 8;7419-7424, 2015.
30. Loeys B. The search for genotype/phenotype correlation in Marfan syndrome: to be or not to be? Eur Heart J 37;3291-3293, 2016.
31. Liu W., Schrijver I., Brenn T., Furthmayr H., Francke U. Multi-exon deletions of the FBN1 gene in Marfan syndrome. BMC Med Genet 2;11, 2001.
32. Robinson P.N., Booms P., Katzke S., Ladewig M., Neumann L., Palz M., Pregla R., Tiecke F., Rosenberg T. Mutations of FBN1 and genotype-phenotype correlations in Marfan syndrome and related fibrillinopathies. Hum Mutat 20;153-61, 2002.
33. Pees C., Michel-Behnke I., Hagl M., Laccone F., Detection of 15 novel mutations in 52 children from 40 families with the Marfan or Loeys-Dietz syndrome and phenotype-genotype correlations. Clin. Genet 86;552-557, 2014.
34. Putnam EA, Cho M, Zinn AB, *et al*. Delineation of the Marfan phenotype associated with mutations in exons 23–32 of the FBN1 gene. Am J Med Genet 1996;62:233–42.
35. Tiecke F., Katzke S., Booms P., Robinson P.N., Neumann L., Godfrey M., et. al. Classic, atypically severe and neonatal Marfan syndrome: twelve mutations and genotype-phenotype correlations in FBN1 exons 24-40. Eur J Hum Genet 1;13-21, 2001.
36. Schrijver I., Liu W., Brenn T., Furthmayr H., Francke U. Cysteine substitutions in epidermal growth factor-like domains of fibrillin-1: distinct effects on biochemical and clinical phenotypes. Am J Hum Genet 65;1007-20, 1999.

37. Loeys B., De Backer J., Van Acker P., Wettinck K., Pals G., Nuytinck L., Coucke P., De Paepe A. Comprehensive molecular screening of the FBN1 gene favors locus homogeneity of classical Marfan syndrome. Hum Mutat 24;140–146, 2004.
38. Rommel K., Karck M., Haverich A., von Kodolitsch Y., Rybczynski M., Muller G. Identification of 29 novel and nine recurrent fibrillin-1 (FBN1) mutations and genotype–phenotype correlations in 76 patients with Marfan syndrome. Hum Mutat 26;529–39, 2005.
39. Faivre L, Collod-Beroud G, Loeys BL, Child A, Binquet C, Gautier E, Callewaert B, Arbustini E, Mayer K, Arslan-Kirchner M, Kiotsekoglou A, Comeglio P, Marziliano N, Dietz HC, Halliday D, Beroud C, Bonithon-Kopp C, Claustres M, Muti C, Plauchu H, Robinson PN, Ades LC, Biggin A, Benetts B, Brett M, Holman KJ, De Backer J, Coucke P, Francke U, DePaepe A, Jondeau G, Boileau C. Effect of mutation type and location on clinical outcome in 1,013 probands with Marfan syndrome or related phenotypes and FBN1 mutations: an international study. Am J Hum Genet 2007;81:454–66.
40. Baudhuin L.M., Kotzer K.E., Lagerstedt S.A. Increased frequency of FBN1 truncating and splicing variants in Marfan syndrome patients with aortic events. Genet Med 17;177-87, 2015.
41. Schrijver I., Liu W., Brenn T, Furthmayr H., Francke U. Cysteine substitutions in epidermal growth factor-like domains of fibrillin-1: distinct effects on biochemical and clinical phenotypes. Am J Hum Genet 65;1007-20, 1999.
42. Schulz, G.E., Schirmer, R.H. (1979). Principles of Protein Structure. New York, NY, USA: Springer-Verlag, pp. 1–16. DOI: 10.1007/978-1-4612-6137-7
43. Reinhardt, D.P., Ono, R.N., Notbohm, H., Müller, P.K., Bächinger, H.P., Sakai, L.Y. (2000). Mutations in calcium-binding epidermal growth factor modules render fibrillin-1 susceptible to proteolysis. A potential disease-causing mechanism in Marfan syndrome. *Journal of Biological Chemistry*, 275(16), 12339–12345. DOI: 10.1074/jbc.275.16.12339
44. Kirschner, R., Hubmacher, D., Iyengar, G., Kaur, J., Fagotto-Kaufmann, C., Brömme, D., Bartels, R., Reinhardt, D.P. (2011). Classical and neonatal Marfan syndrome mutations in fibrillin-1 cause differential protease susceptibilities and protein function. *Journal of Biological Chemistry*, 286(37), 32810–32823. DOI: 10.1074/jbc.M111.221804

45. Boileau C., Jondeau G., Mizuguchi T., Matsumoto N. Molecular genetics of Marfan syndrome. Curr Opin Cardiol 194-200, 2005.
46. Katzke S., Booms P., Tiecke F., Palz M., Pletschacher A., Turkmen S., et al. TGGE screening of the entire FBN1 coding sequence in 126 individuals with Marfan syndrome and related fibrillinopathies. Hum Mutat 20;197–208, 2002.
47. Korkko J., Kaitila I., Lonnqvist L., Peltonen L., Ala-Kokko L. Sensitivity of conformation sensitive gel electrophoresis in detecting mutations in Marfan syndrome and related con- ditions. J Med Genet 39;34–41, 2002.
48. Judge D.P., Biery N.J., Keene D.R., Geubtner J., Myers L., Huso D.L., Sakai L.Y., Dietz H.C. Evidence for a critical contribution of haploinsufficiency in the complex pathogenesis of Marfan syndrome. J Clin Invest 114;172–181, 2004..
49. Hutchinson S., Furger A., Halliday D., Judge D.P., Jefferson A., Dietz H.C., et al. Allelic variation in normal human FBN1 expression in a family with Marfan syndrome: a potential modifier of phenotype? Hum Mol Genet 12; 2269–2276, 2003.
50. Aubart M., Gross M.S., Hanna N., Zabot M.T., Sznajder. M, Detaint D., Gouya L, et al. The clinical presentation of Marfan syndrome is modulated by expression of wild-type FBN1 allele. Hum Mol Genet 24;2764–2770, 2015.
51. Aoyama T., Francke U., Gasner C., Furthmayr H.. Fibrillin abnormalities and prognosis in Marfan syndrome and related disorders. Am J Med Genet 58;169–176, 1995.
52. Franken R., Teixido-Tura G., Brion M., Forteza A., Rodriguez Palomares J., Gutierrez L., Garcia Dorado D., Pals G., Mulder BJ., Evangelista A. Heart. 103:1795-1799, 2017.

Figure 1

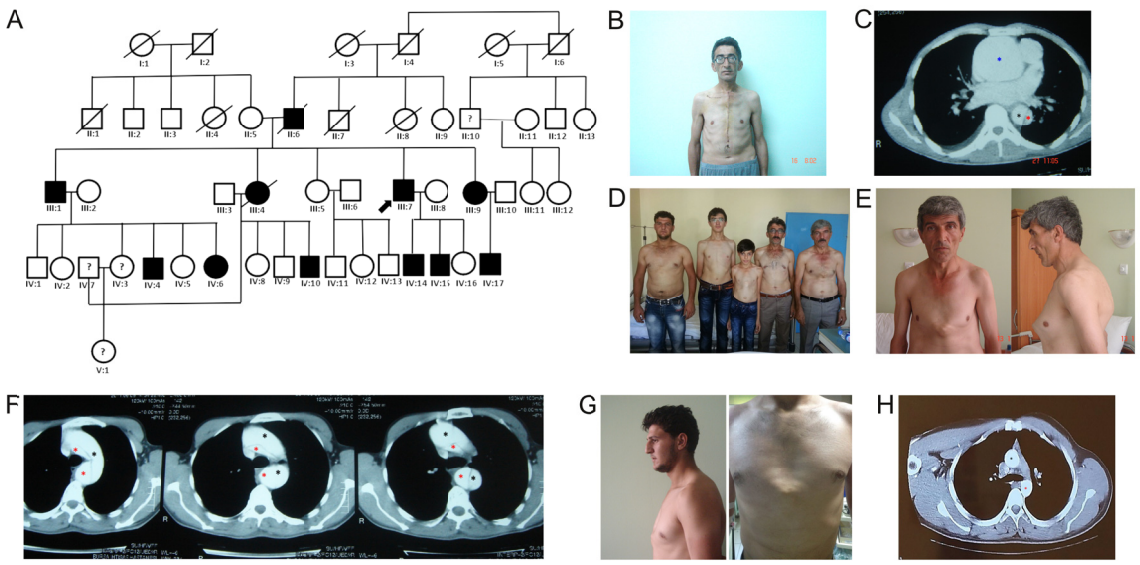

Figure 2

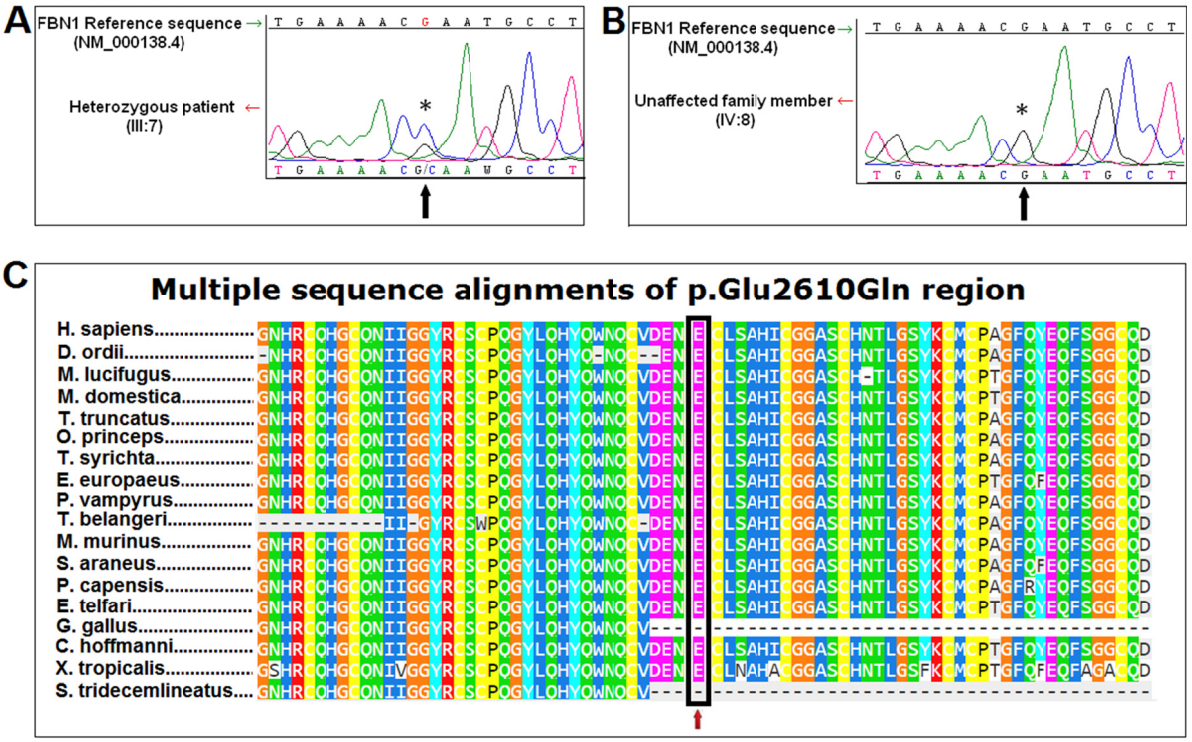

Figure 3

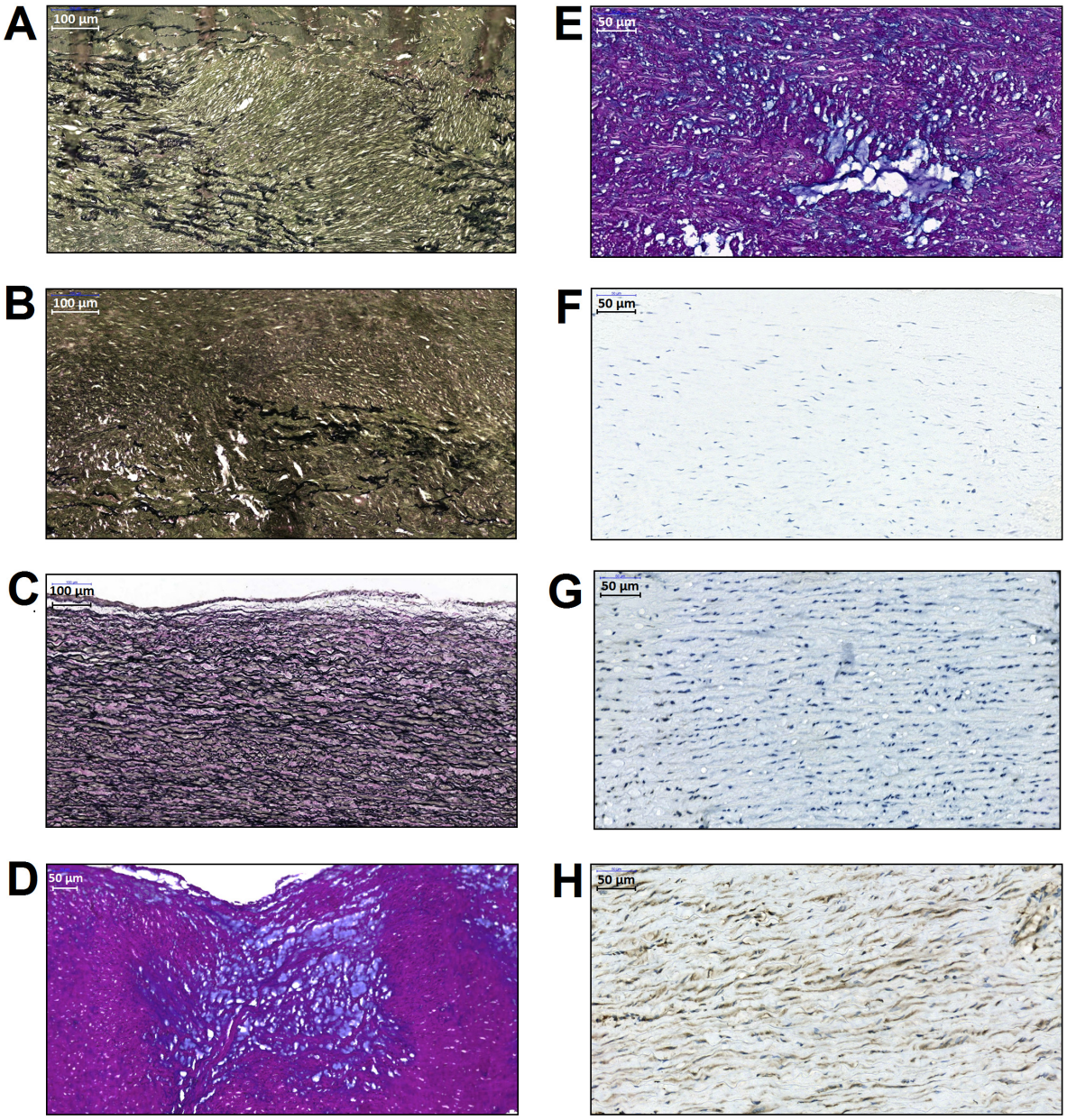

Figure 4a

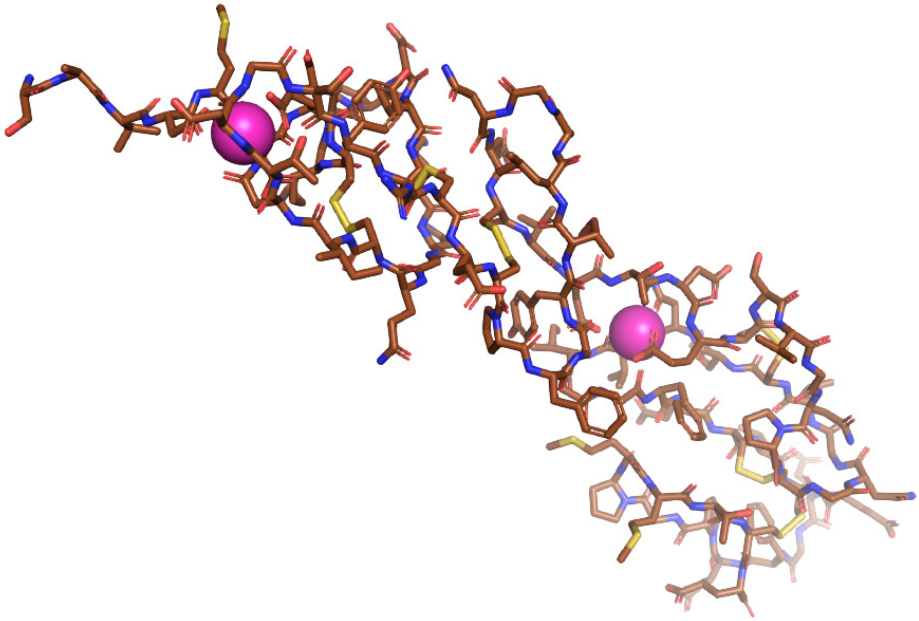

Figure 4b

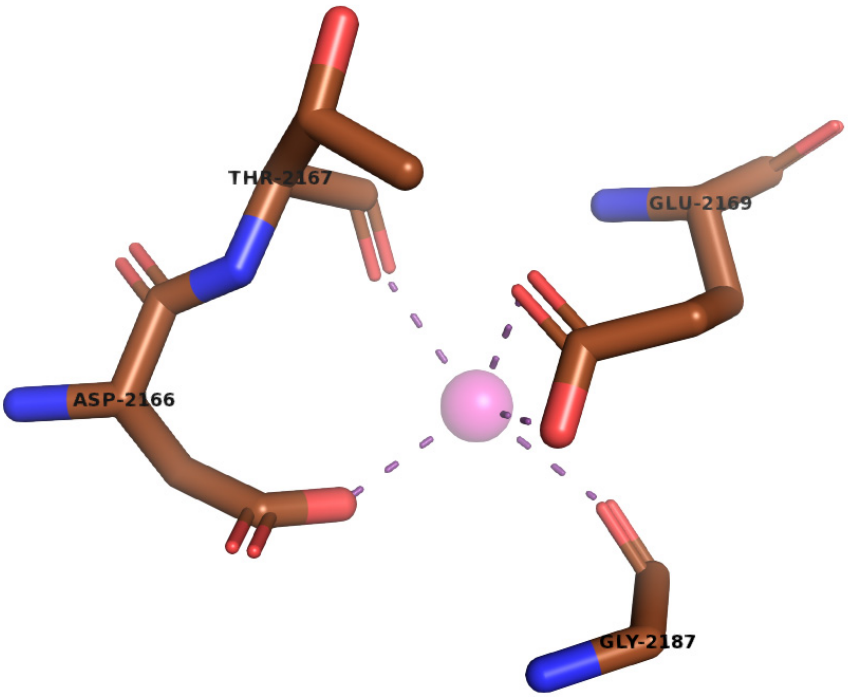

Figure 4c

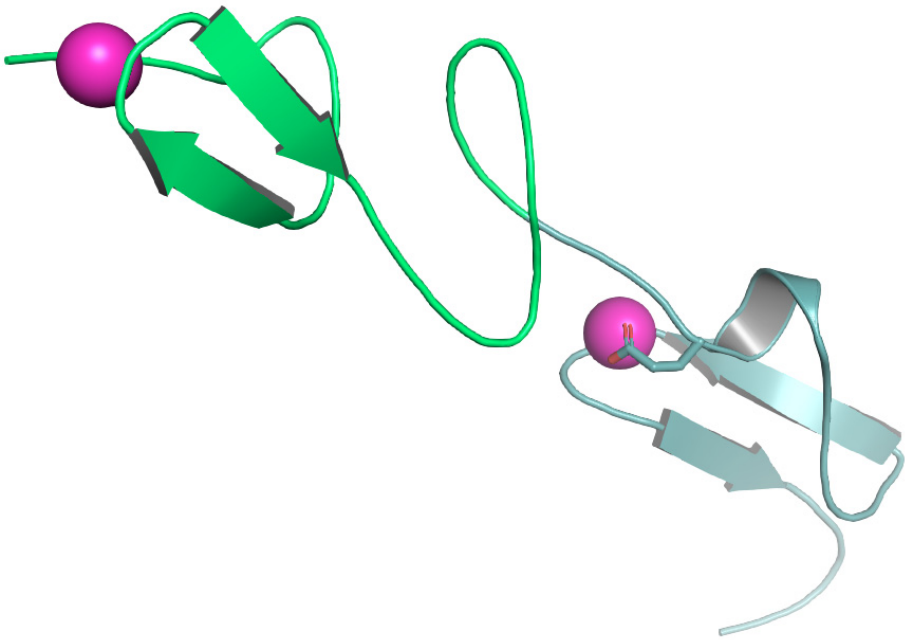

Figure 4d